Cellular stress from excitatory neurotransmission contributes to cholesterol loss in hippocampal neurons aging in vitro

Alejandro O. Sodero[a,b], Carina Weissmann[b], Maria Dolores Ledesma[c,*], Carlos G. Dotti[a,b,*]

[a] *VIB Department of Molecular and Developmental Genetics, Katholieke Universiteit Leuven, Leuven, Belgium*
[b] *Department of Human Genetics, Katholieke Universiteit Leuven, Leuven, Belgium*
[c] *Department of Molecular Neurobiology, Centro de Biología Molecular Severo Ochoa (CSIC-UAM), Madrid, Spain*

Abstract

After approximately 3 weeks in vitro, hippocampal neurons present many of the typical hallmarks accompanying neuronal aging in vivo, including accumulation of reactive oxygen species (ROS), lipofuscin granules, heterochromatic foci, and activation of the Jun N-terminal protein kinase (pJNK) and p53/p21 pathways. In addition, hippocampal neurons in vitro undergo a gradual loss of cholesterol, which is important for the activation of the prosurvival tyrosine kinase receptor TrkB. Here, we used the hippocampal in vitro system to investigate the possible cause of age-accompanying cholesterol loss. We report that cholesterol loss during in vitro aging is paralleled by upregulation and translocation to the neuronal surface of cholesterol-24-hydroxylase (Cyp46), the enzyme responsible for cholesterol removal from neurons. Chronic reduction of electrical activity diminished cholesterol loss in aged neurons and precluded the upregulation of cholesterol-24-hydroxylase. In agreement with a cause-effect relationship, stimulation of excitatory neurotransmission in young neurons led to cholesterol loss. Mechanistically, N-methyl-D-aspartate (NMDA)-mediated excitatory neurotransmission leads to cholesterol loss through generation of reactive oxygen species derived from the activation of the stress-responsive enzyme NADPH oxidase. Supporting the relevance of the in vitro data, reduced cholesterol was also detected in synaptic membranes from old mice brains. Furthermore, excitatory neurotransmission via the nicotinamide adenine dinucleotide phosphate (NADPH)-oxidase pathway induced cholesterol loss in purified brain synaptosomes. The current studies highlight excitatory neurotransmission as 1 of the mechanisms involved in cholesterol loss during aging.
© 2011 Elsevier Inc. All rights reserved.

Keywords: Aging; Cultured hippocampal neurons; Cholesterol; Cyp46; NMDA; Excitatory neurotransmission; Reactive oxygen species

1. Introduction

Understanding how neurons survive in the aged brain, where the levels of prosurvival neurotrophins like brain-derived neurotrophic factor (BDNF) are low (Gooney et al., 2004; Hattiangady et al., 2005; Shetty et al., 2004), but the burden of stress side-products accumulated during life is high (Dröge and Schipper, 2007; Serrano and Klann, 2004), is a major challenge. Recently, a gradual and persistent loss of cholesterol from the neuronal plasma membrane has been shown to activate the survival pathway mediated by TrKB receptor in aged cultured neurons and aged brains (Martin et al., 2008). This activation is independent of the TrKB binding neurotrophin BDNF, but dependent on the upregulation of the catabolic enzyme cholesterol-24-hydroxylase (Cyp46) (Martin et al., 2008). The conversion of cholesterol into 24S-hydroxy-cholesterol by this enzyme is quantitatively the most important mechanism to eliminate cholesterol from the brain (Björkhem et al., 1998; Lütjohann et al., 1996). However, Cyp46 transcriptional regulation is limited, being oxidative stress the only factor, described until now, able to influence its expression (Ohyama et al., 2006).

In this work, we focused on determining the mechanisms responsible for Cyp46 upregulation/cholesterol loss during aging. We hypothesized that accumulation of reactive oxygen

* Corresponding author at: K.U. Leuven, Herestraat 49, 3000, Leuven, Belgium. Tel.: +32 16 330519; fax: +32 16 330522.
  E-mail address: carlos.dotti@med.kuleuven.be (C.G. Dotti).
* Alternate corresponding author at: Centro de Biología Molecular Severo Ochoa, Nicolas Cabrera 1, 28049 Madrid, Spain. Tel.: +34 9119 64547; fax: +34 9119 64420.
  E-mail address: dledesma@cbm.uam.es (M.D. Ledesma).

species (ROS) due to physiological activities plays a preponderant role. Most conspicuous among the physiological activities leading to ROS load is synaptic transmission. In fact, neurotransmission implies the use of large amounts of energy in the form of adenosine triphosphate (ATP) (Attwell and Iadecola, 2002) and transient rises in intracellular Ca^{2+} (Zucker, 1999), both leading to the generation of free radicals (Kamsler and Segal, 2004). We now show that synaptic activity significantly contributes to age-related cholesterol loss through the activation of Cyp46, and that this process crucially depends on the generation of oxidative stress.

2. Methods

2.1. Primary hippocampal cultures

Primary cultures were prepared from Wistar rat fetuses at embryonic day 19 as described in Kaech and Banker (2006). For biochemical analysis, 3-cm plastic dishes were coated with 0.1 mg/mL of poly-L-lysine (PLL) and dissociated cells were plated at a density of 150,000 per dish. Neurons were grown in minimal essential medium with N2 supplement (MEM-N2), at 37 °C and under 5% CO_2. For microscopy experiments, cells were plated on glass coverslips coated with 1 mg/mL of PLL and grown in minimal essential medium with N2 supplement with a supporting astroglial monolayer underneath.

2.2. Drugs and treatments

Hippocampal neurons in culture were treated with the sodium channel blocker tetrodotoxin (TTX, Sigma, St Louis, MO) or the NADPH oxidase inhibitor apocynin (APC, Calbiochem), in order to reduce synaptic activity or oxidative stress, respectively. To reach a sustained inhibition of the synaptic activity through the aging process, 1 μM TTX was added in the medium at 14, 16, 18, and 20 days in vitro (DIV). To reduce oxidative stress in cultured neurons, 0.5 mM APC was added at 14 DIV and kept in the medium until 22 DIV. Experiments after TTX or APC treatments were performed at 22 DIV.

Oxidative stress was induced by incubation of 10 DIV neurons with 5 μM tert-butyl-hydroperoxide (TBHP, Sigma) for 30 minutes.

Spontaneously active neurons of 14 DIV were incubated for 30 minutes with 10 μM N-methyl-D-aspartate (NMDA, Sigma). To block NMDA-induced cholesterol loss, 14 DIV neurons were treated for 10 minutes with 10 μM DL-2-amino-5-phosphonopentanoic acid (AP-5, Fluka) and then challenged with 10 μM NMDA for an additional 30 minutes, in presence of the NMDA receptor antagonist.

To block NMDA-induced oxidative stress, 14 DIV neurons were treated for 30 minutes with 0.5 mM APC and then challenged with 10 M μM NMDA for additional 30 minutes, in presence of the NADPH oxidase inhibitor.

2.3. Membrane purification and cholesterol detection in hippocampal cultures

Hippocampal neurons were scraped in 25 mM 2-(N-morpholino)ethanesulfonic acid (MES) buffer (pH 7.0) containing 2 mM ethylenediaminetetraacetic acid (EDTA) and protease inhibitor cocktail (Roche). Cells were lysed through a 22-gauge needle and centrifuged at 0.5g for 10 minutes to eliminate nuclei. Then, the supernatant was centrifuged at 100,000g for 1 hour to obtain the membrane fraction. Membrane pellets were resuspended in phosphate-buffered saline (PBS) (137 mM NaCl, 2.7 mM KCl, 10 mM Na_2HPO_4, and 1.76 mM KH_2PO_4; pH 7.4) containing 0.2% sodium dodecyl sulfate (SDS), and the protein concentration was determined using the Bio-Rad Protein Microassay.

Cholesterol levels were assessed by fluorometric detection (Molecular Probes, Invitrogen) in samples containing the same amount of protein. Briefly, cholesterol was oxidized by cholesterol oxidase to yield peroxide and the corresponding ketone. Peroxide was then detected using 10-acetyl-3,7-dihydroxyphenoxazine. This compound, in presence of horseradish peroxidase, reacts with peroxide to produce highly fluorescent resorufin.

2.4. Western blotting

Equivalent amounts of protein for each sample were resolved by 12% SDS-polyacrylamide gel electrophoresis (PAGE) and transferred to a nitrocellulose membrane. The blocking step was performed in 5% milk in Tris-buffered saline with 0.1% Tween 20 (TBS-T) for 1 hour. Then, membranes were incubated overnight at 4 °C with the corresponding primary antibodies. The day after, blots were incubated with horseradish peroxidase-linked secondary antibodies (1: 10,000; Zymed Laboratories, Invitrogen) and developed using chemiluminescence detection (ECL, Amersham). Images were taken using a Fujifilm LAS-3000 system and quantified with ImageJ 1.37v software (NIH, USA).

The following primary antibodies were used: rabbit polyclonal anti Cyp46 (1:2000, provided by Dr D.W. Russell, University of Texas Southwestern Medical Center, Dallas, TX), mouse monoclonal anti Rho-A (1:250; Santa Cruz), and mouse monoclonal anti α-tubulin (1:10,000; Calbiochem).

2.5. Cell surface biotinylation

Biotinylation of plasma membrane Cyp46 was performed using a water soluble, membrane impermeable, and thiol-cleavable biotin. Hippocampal cultures were washed with ice-cold PBS and incubated with 50 μg/mL EZ-link Sulfo-NHS-Biotin (Pierce) for 30 minutes at 4 °C. The excess of biotin was later quenched by washing 3 times with 20 mM glycine. Then, cells were lysed in STEN-lysis buffer (50 mM TRIS, 150 mM NaCl, 2 mM EDTA, 1% Triton X-100 and 1% NP-40; pH 7.6) and biotinylated cell surface proteins were pulled down with streptavidin-Sepharose beads (GE Healthcare). The protein present at the cell sur-

face was detected by western immunoblotting. Quantifications were performed using ImageJ software. The amount of surface Cyp46 (pull-down) was normalized to the amount of total Cyp46 (input) for each age group, and then the percent of change was calculated.

2.6. Quantitative PCR analysis

Ribonucleic acid (RNA) samples were prepared from hippocampal neurons grown in culture using the RNeasy® plus Mini Kit (Qiagen). Then, 500 ng of total RNA were subjected to reverse transcription using the Revert Aid™ H Minus First Strand complementary DNA (cDNA) Synthesis Kit (Fermentas). Afterward, cDNA was used as template for real-time polymerase chain reaction (PCR) analysis based on the SYBR Green PCR Master Mix assay with the ABI PRISM 7000 Sequence Detection System (Applied Biosystems). Real-time PCR primers were designed using Primer-Express software (Applied Biosystems). The expression of the genes of interest (*Cyp46A1* or *p47phox*) was normalized using β_2-microglobulin (*B2MG*) as housekeeping gene, in order to avoid differences due to possible RNA degradation or different reverse transcription efficacy. The relative expression levels were calculated using the $\Delta\Delta$Ct method.

2.7. Detection of proteins by immunofluorescence

Neurons grown on PLL-coated glass coverslips were fixated with 4% p-formaldehide, permeabilized with 0.1% Triton x-100 and treated with blocking solution (2% fetal calf serum, 2% bovine serum albumin, and 0.2% fish skin gelatin). Then, neurons were incubated with the primary antibody for 60 minutes at room temperature. Finally, neurons were exposed to the secondary antibody (1/10,000; Alexa Fluor) for 30 minutes.

The following primary antibodies were used: mouse anti phosphorylated Tau, epitope paired helical filament helical filament (PHF)-1 (1/50; Pierce), mouse monoclonal anti acetylated-tubulin (1/1,000; Sigma-Aldrich) and rabbit
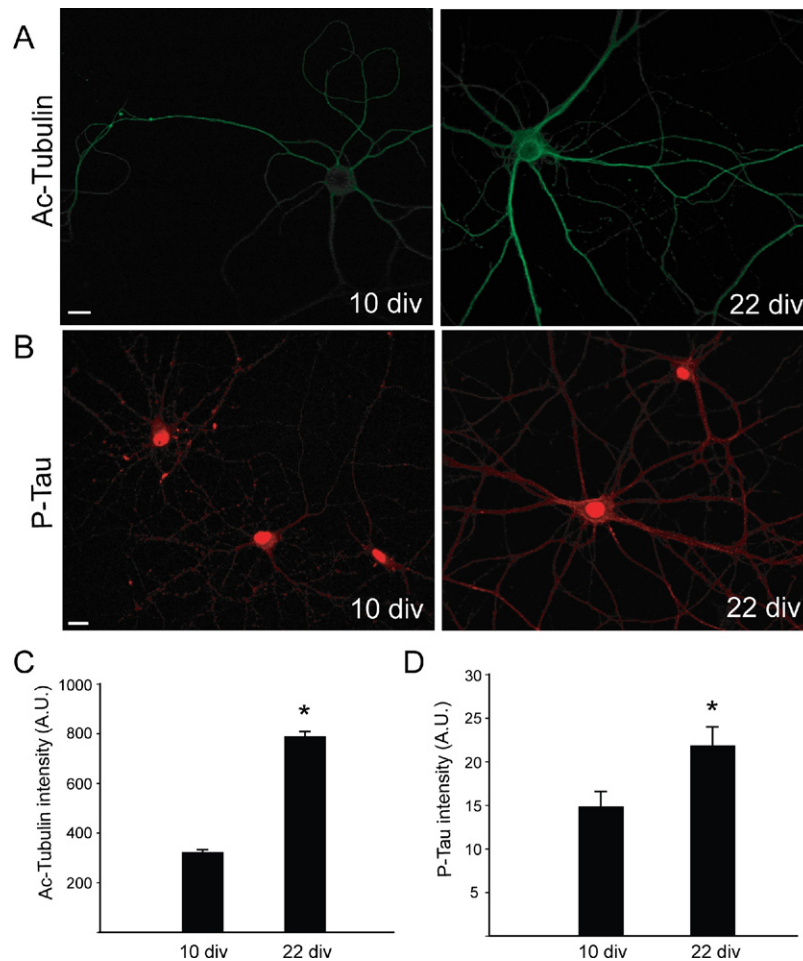

Fig. 1. Senescence signs in hippocampal neurons aging in vitro. (A) Representative confocal images comparing tubulin acetylation in 10 and 22 days in vitro (DIV) hippocampal neurons. Scale bar: 10 μm. (B) Representative confocal images comparing Tau phosphorylation in 10 and 22 DIV hippocampal neurons, by using an antibody that recognizes the PHF-1 epitope of the Tau molecule only when it is phosphorylated. Scale bar: 10 μm. (C) Quantification of the acetylated tubulin signal in 10 and 22 DIV hippocampal neurons. The intensity of 10 dendritic segments, from the soma to the distal part, was analyzed in different neurons and the average intensity of all the segments was calculated (see methods section for details). (D) Average intensity of the phosphorylated Tau signal analyzed in randomly selected dendrite segments of 10 and 22 DIV hippocampal neurons.

polyclonal p47phox (1/100; Santa Cruz). Phosphorylated Tau and acetylated tubulin images were taken using a Nikon confocal microscope, and p47phox images were taken using an epi-fluorescence Olympus microscope.

MetaMorph software was used for quantitative analysis of the intensity of the acetylated-tubulin signal along dendrites. The acquired images, using the same settings, were corrected for background: the average background calculated from several regions that did not contain labeled dendrites was subtracted and this corrected image was used for analysis. Regions of interest were highlighted and selected in the MetaMorph program with the "autothreshold bright objects" function. To quantify the fluorescence in the cellular processes of the stained cells, a 4-pixel-wide line was drawn medially along the dendrites. A "segment" function was then applied to divide the lines in 10-pixel long regions, and the average fluorescence signal was determined in each portion. For PHF-1-stained cells, the average signal intensity along dendrites was calculated using the Neuron J plugin of ImageJ software. In this case, lines of 10 to 20 μm were traced with the software along dendrites, and the average intensity was measured.

2.8. Detection of reactive oxygen species (ROS)

Neurons grown on PLL-coated glass coverslips were treated with 10 μM dihydrorhodamine (DHR; Molecular Probes) in conditioned medium for 20 minutes and then fixed with 4% p-formaldehide. The fluorescent product, rhodamine-123, was detected using a Nikon confocal microscope.

2.9. Isolation of mouse synaptosomes

Synaptosomes were isolated from young (4 months old) and old (24 months old) adult C57BL/6J male mice using Percoll gradients (Dunkley et al., 1988). Briefly, animals were killed by cervical dislocation, their brains were quickly removed, cerebellum and olfatory bulb were dissected out, and the hemispheres were put into ice-cold buffer a (320 mM sucrose, 1 mM EDTA, protease inhibitor cocktail; pH 7.4). After homogenization with 8 strokes in a Glass-Teflon, the homogenate was centrifuged at 1000g for 10 minutes. The obtained supernatant (S1) was loaded on top of a gradient constituted by 4 phases of 3%, 10%, 15%, and 23% Percoll and centrifuged at 25,000g for 10 minutes. Synaptosomes were taken with a Pasteur pipette from the interphase 15%–23%, diluted in PBS and centrifuged at 100,000g for 1 hour to obtain synaptosomal membranes. Then, membranes were resuspended in PBS containing 0.2% SDS and cholesterol levels were assessed by fluorometric detection (Molecular Probes, Invitrogen) in samples containing the same amount of protein.

2.10. Isolation and stimulation of rat synaptosomes

Crude synaptosomes were prepared from 3-month-old male Wistar rats following an established protocol (Schubert et al., 2006). Briefly, brains were quickly removed, olfactory bulb and cerebellum were dissected out, and both hemispheres were put into ice-cold buffer a (320 mM sucrose, 4 mM (4-(2-hydroxyethyl)-1-piperazineethanesulfonic acid (HEPES) and protease inhibitor cocktail; pH 7.4).
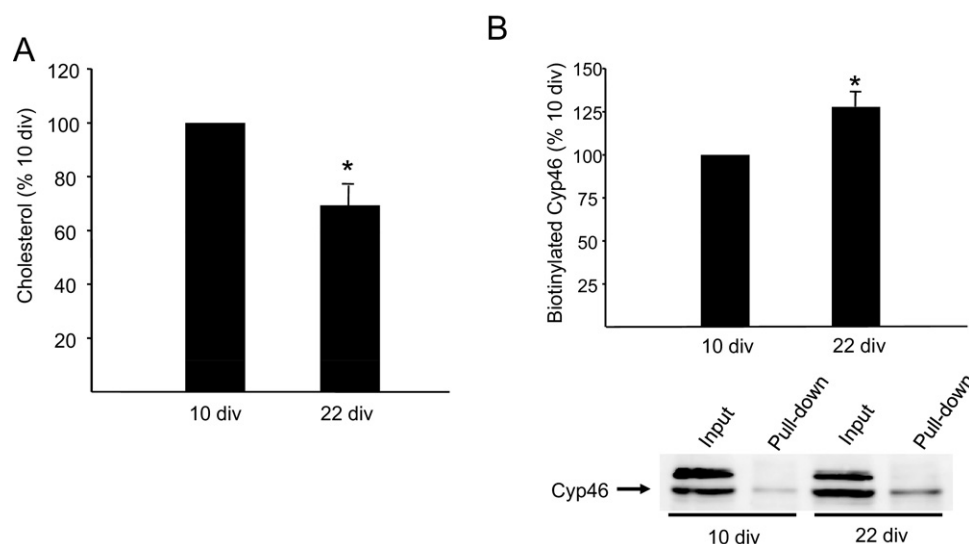

Fig. 2. Cholesterol loss in aged hippocampal neurons is accompanied by increased expression of cholesterol-24-hydroxylase (Cyp46) and translocation of the enzyme to the cell surface. (A) Membrane cholesterol content in 22 days in vitro (DIV) compared with 10 DIV hippocampal neurons; *$p < 0.05$ ($n = 9$). (B) Levels of Cyp46 at the neuronal plasma membrane detected by cell surface biotinylation in aged hippocampal neurons, compared with young neurons. Biotinylated, cell surface Cyp46 (pull-down) was normalized to the amount of total Cyp46 in the cell lysate (input: half of the protein amount used in the streptavidin pull-down). Then, the percentage of change of surface Cyp46 was calculated between young and old neurons. A representative western blot is shown below the graph. Upregulation experiments in our laboratory have confirmed that the specific band for Cyp46 is the lower one recognized by the antibody, indicated by an arrow; *$p < 0.05$ ($n = 3$). Graphs in (A) and (B) represent mean ± standard error of the mean (SEM).

After homogenization with 8 strokes in a Glass-Teflon, the homogenate was centrifuged at $1400g$ for 10 minutes (P1). The supernatant S1 was kept. The homogenate (P1) was then homogenized in buffer A and centrifugated at $700g$ for 10 minutes (P2). The obtained supernatant S2 and S1 were pooled and centrifugated at $13,800g$ for 10 minutes to yield the crude synaptosomal pellet (P3). The synaptosomal pellet (P3) fraction was resuspended in 5 mM KCl buffer (130 mM NaCl, 5 mM KCl, 2.2 mM $CaCl_2$, 4 mM $NaHCO_3$, 5.6 mM glucose, 0.5 mM Na_2HPO_4, 0.4 mM KH_2PO_4, and 10 mM HEPES; pH 7.4). After 30 minutes of stabilization at 37 °C, synaptosomal fractions containing 2 mg of protein were incubated with 5 mM KCl buffer or 55 mM KCl buffer (80 mM NaCl, 55 mM KCl, 2.2 mM $CaCl_2$, 4 mM $NaHCO_3$, 5.6 mM glucose, 0.5 mM Na_2HPO_4, 0.4 mM KH_2PO_4 and 10 mM HEPES; pH 7.4) for 15 minutes. Stimulation was stopped by placing the samples in ice and adding 32 μL of 1 M $MgCl_2$.

When synaptosomes were stimulated with 10 μM NMDA (30 minutes), 5 mM KCl buffer was used.

For blocking oxidative stress 0.5 mM APC was added 15 minutes before the depolarization with 55 mM KCl.

After stimulation, synaptosomal membranes were obtained by centrifugation of the fractions at $100,000g$ and 4 °C for 1 hour. Membrane pellets were resuspended in PBS containing 0.2% SDS. Then, cholesterol levels were assessed by fluorometric detection (Molecular Probes, Invitrogen) in samples containing the same amount of protein.

2.11. Detection of apoptosis

Hippocampal neurons grown on PLL-coated glass coverslips were treated with TTX as described above and the number of apoptotic cells was evaluated at 22 DIV (nontreated and TTX-treated). Cells were fixed with 4% p-formaldehide and DNA fragmentation was detected using the DeadEnd™ Fluorometric TUNEL System (Promega, Madison, WI) following the manufacturer's instructions.

2.12. Statistical analysis

Comparisons between groups were performed with the Student t test. Differences were considered significant when $p < 0.05$.
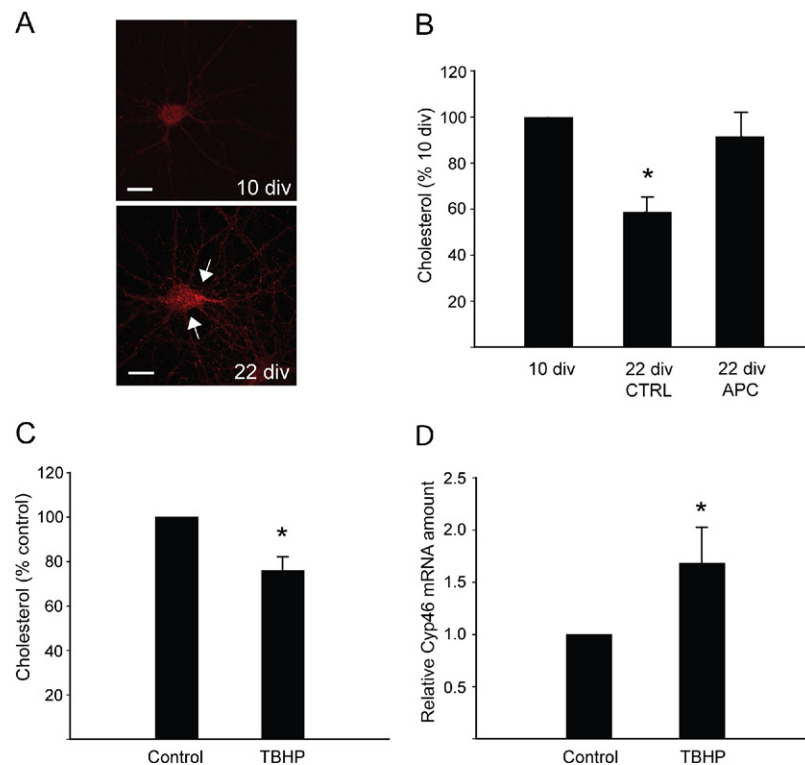

Fig. 3. Reactive oxygen species (ROS) are involved in aged-related cholesterol loss. (A) Representative confocal images showing a higher intracellular accumulation of ROS measured by dihydrorhodamine staining (red dots indicated by arrows) in 22 days in vitro (DIV) compared with 10 DIV hippocampal neurons. (B) Membrane cholesterol content in 22 DIV hippocampal neurons, treated or not with 0.5 mM apocynin (APC), compared with 10 DIV neurons. The NADPH oxidase inhibitor apocynin (APC) was added at day 14 and kept in the medium until day 22 in order to reduce the production of superoxide; *$p < 0.05$. (C) Membrane cholesterol content in 10 DIV hippocampal neurons treated for 30 minutes with 5 μM tert-butyl-hydroperoxyde (TBHP), compared with nontreated neurons; *$p < 0.05$. (D) Relative amount of cholesterol-24-hydroxylase (Cyp46) mRNA assessed by quantitative polymerase chain reaction (PCR) in 10 DIV hippocampal neurons treated with 5 μM tert-butyl-hydroperoxyde (TBHP) for 30 minutes, compared with control neurons; *$p < 0.05$. Graphs in (B), (C), and (D) represent mean ± standard error of the mean (SEM) from at least 3 independent experiments.

3. Results

3.1. Increased expression and cell surface levels of Cyp46 in hippocampal neurons aging in vitro

Aging is characterized by a series of hallmarks, including the presence of cumuli of ROS in mitochondria (Chen et al., 1998), lipofuscin granules (Gray and Woulfe, 2005; Szweda et al., 2003), high activity of Jun N-terminal protein kinase/ mitogen-activated protein kinase (JNK/MAP) kinase (Pham et al., 2005) and upregulation of p53 and p21 (Wu et al., 2004). In a recent publication, we showed that similar changes take place in long term cultured hippocampal neurons (Martin et al., 2009). In further agreement with these results, it was also shown that aging hippocampal cultures present increased protein oxidation, creatine kinase expression, and calcium channel density, justifying the use of this system as a suitable model to study brain aging (Aksenova et al., 1999; Kuroda et al., 1995; Porter et al., 1997). In any event, in order to further prove the suitability of this system, we here show that cultured hippocampal neurons undergo a time-associated increase in tubulin acetylation (Fig. 1A and 1C), similarly to the in vivo situation (Fifkova and Morales, 1992; Perez et al., 2009). Another proof that embryonic hippocampal neurons age in vitro is the time-associated increase in the phosphorylation of the microtubule-associated protein Tau, assessed with an antibody that recognizes the PHF-1 epitope only when it is phosphorylated (Fig. 1B and 1D). Increased Tau phosphorylation in vitro matches previous observations in aged human brains (Pikkarainen et al., 2009; Uboga and Price, 2000), in Alzheimer's disease patient brains (An et al., 2003; Small and Duff, 2008), and in mouse models of senescence (Tomobe and Nomura, 2009). The observed changes cannot be attributed to increased apoptosis, as this does not vary significantly between the time-points analyzed (11.5 ± 3.7% and 15.2 ± 4.4%, for 14 and 22 DIV neurons, respectively). Hence, we find it reasonable to conclude that after 22 DIV embryonic hippocampal neurons in culture have acquired several biochemical characteristics of the aged neuron in situ.

Hippocampal neurons from old mice are characterized by a paucity of cholesterol (Martin et al., 2008). Fig. 2A shows that the same occurs in hippocampal neurons in vitro: 22 DIV neurons present a significant reduction (33.4 ± 7.7%) in the amount of membrane cholesterol compared with 10 DIV neurons. Reduced cholesterol in aged neurons can be the consequence of reduced synthesis or increased hydroxylation and further elimination. In a PCR-based study we have recently shown that old neurons present increased transcription of the cholesterol-24-hydroxylase gene, without changes in the levels of the synthetic or transport enzymes (Martin et al., 2008), indicating that the loss of this sterol in aged cells is largely due to increased removal. Quantitative PCR confirmed that 22 DIV neurons present higher Cyp46 messenger RNA (mRNA) levels than 10 DIV neurons (Fig. 6B). Western blotting revealed a parallel increase in protein levels (Fig. 6C). Because most of the cellular cholesterol is found in the plasma membrane (Fisher, 1976; Mondal et al., 2009; Wood et al., 2002), its reduced levels in aged neurons should be accompanied by an increase in the surface appearance of the cholesterol catabolic enzyme. Consistently, cell surface biotinylation experiments showed a significant increase of Cyp46 at the plasma membrane of old neurons compared with young ones (27.7 ± 8.7%; Fig. 2B).

3.2. ROS induce cholesterol loss and Cyp46 upregulation in hippocampal neurons aging in vitro

In vitro studies showed that ROS control the transcriptional activity of the Cyp46 gene (Ohyama et al., 2006). Hence, we tested if ROS accumulation during hippocampal aging in vitro played a role in Cyp46 activation in these cells. Because Cyp46 is mainly responsible for cholesterol
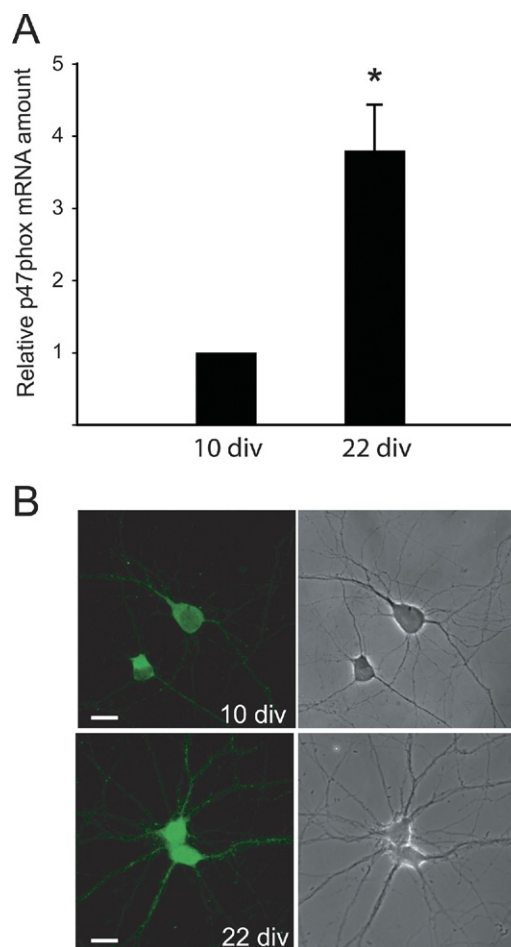
Fig. 4. Reactive oxygen species (ROS) increase in aged hippocampal neurons involves the p47phox subunit of NADPH oxidase. (A) Relative amount of p47phox mRNA assessed by quantitative polymerase chain reaction (PCR) in 22 days in vitro (DIV) compared with 10 DIV hippocampal neurons; *$p < 0.05$ ($n = 3$). (B) Representative epi-fluorescence images showing higher expression of p47phox in 22 DIV compared with 10 DIV hippocampal neurons. Scale bar: 10 μm.
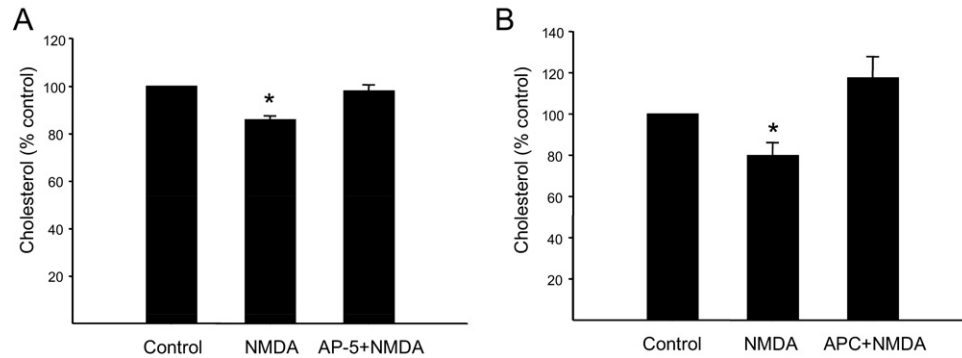
Fig. 5. Cholesterol loss is mediated by N-methyl-D-aspartate (NMDA) receptors and involves the generation of reactive oxygen species (ROS). (A) Membrane cholesterol content in 14 days in vitro (DIV) hippocampal neurons stimulated with 10 μM NMDA for 30 minutes, in absence (NMDA) or presence of 10 μM DL-2-amino-5-phosphonopentanoic acid (AP-5; AP-5+NMDA), compared with nontreated neurons (Control); *$p < 0.05$ ($n = 3$). (B) Membrane cholesterol content in 14 DIV hippocampal neurons stimulated with 10 μM NMDA for 30 minutes in absence or presence of 0.5 mM apocynin (APC; APC+NMDA), compared with nontreated neurons (Control); *$p < 0.05$ ($n = 3$). Graph represents mean $\pm$ standard error of the mean (SEM).

removal, the levels of this sterol were used as read out for Cyp46 activation. Fig. 3A shows an increased accumulation of ROS in 22 DIV neurons compared with 10 DIV neurons. To test the existence of a direct cause-effect relationship between accumulation of ROS and cholesterol loss (see Fig. 2A), we inhibited the NADPH oxidase pathway of ROS generation by treating the neurons with apocynin (APC), from 14 to 22 DIV. APC is a specific NADPH oxidase inhibitor that reduces the production of superoxide in cultured primary neurons (Behrens et al., 2007). Chronic treatment with APC significantly prevented cholesterol loss in aged neurons (Fig. 3B). To further demonstrate the involvement of ROS in cholesterol loss, we induced the generation of ROS in young hippocampal neurons by addition of tert-butyl-hydroperoxide (TBHP). This treatment caused a significant loss of cholesterol ($24.0 \pm 6.0\%$; Fig. 3C), similar to that observed in nontreated old hippocampal neurons. In agreement with a key role of Cyp46 in ROS-mediated cholesterol loss, the same treatment with TBHP increased the mRNA levels of this enzyme (Fig. 3D). Altogether, these results show that cellular ROS are a sufficient and necessary stimulus for neuronal cholesterol loss.

3.3. ROS leads to cholesterol loss via NMDA-mediated NADPH oxidase activation

ROS in cultured hippocampal neurons originate from multiple sources, some inherent to the in vitro condition (i.e., variations in humidity, osmolarity, nutrients, temperature, and gases), others inherent to the physiology of neurons. Among the latter, N-methyl-D-aspartate (NMDA) receptor activation is the primary source of superoxide, via the activation of the NADPH oxidase pathway (Brennan et al., 2009). In agreement with this pathway playing a key role as a source of ROS in our system, the expression levels of p47phox, a subunit required for the functional assembly of NADPH oxidase, were higher in aged neurons, both at the mRNA (Fig. 4A) and protein levels (Fig. 4B). Therefore, we

next tested if NMDA was able to induce cholesterol loss and to which extent this could be due to NADPH oxidase activation. For this, 14 DIV hippocampal neurons were treated for 30 minutes with 10 μM NMDA. This resulted in a significant membrane cholesterol loss, which was abolished in presence of the NMDA receptor antagonist DL-2-amino-5-phosphonopentanoic acid (AP-5) (Fig. 5A). Under similar conditions, addition of the NADPH oxidase inhibitor APC rescued NMDA-induced cholesterol loss (Fig. 5B). These results demonstrate that ROS produced by NADPH oxidase derive from higher levels of excitatory neurotransmission, through activation of NMDA receptors, and are responsible for the cholesterol reduction.

Next, we analyzed to which extent lifelong (in vitro) synaptic transmission participated in cholesterol loss of aged neurons. To test this, hippocampal cultures were incubated with the specific sodium channel blocker tetrodotoxin (TTX) (Urenjak and Obrenovitch, 1996). The treatment was chronic, starting at 14 DIV, a time point at which hippocampal neurons have begun to fire spontaneously (Bacci et al., 1999; Köller et al., 1993), and maintained until 22 DIV. To assure maximum blockage of sodium currents, extra doses of TTX were added every second day. TTX treatment partially prevented age-associated cholesterol loss, which showed a reduction from $29.6 \pm 11.5\%$ to $17.4 \pm 12.2\%$ under conditions of reduced synaptic activity (Fig. 6A). Real-time PCR and western blotting confirmed that TTX also prevented the rise in Cyp46, at the mRNA and protein levels (Fig. 6B and 6C). Moreover, long-term TTX treatment resulted in a clear reduction in the levels of ROS of 22 DIV neurons, compared with untreated controls (Fig. 6D), strongly indicative that one of the sources of ROS leading to Cyp46 activation and cholesterol loss (see Fig. 4) is neurotransmission. That the effect observed in TTX-treated cells was due to diminished neurotransmission is evidenced by the reduced levels of membrane bound RhoA, which has been shown to increase with synaptic transmis-
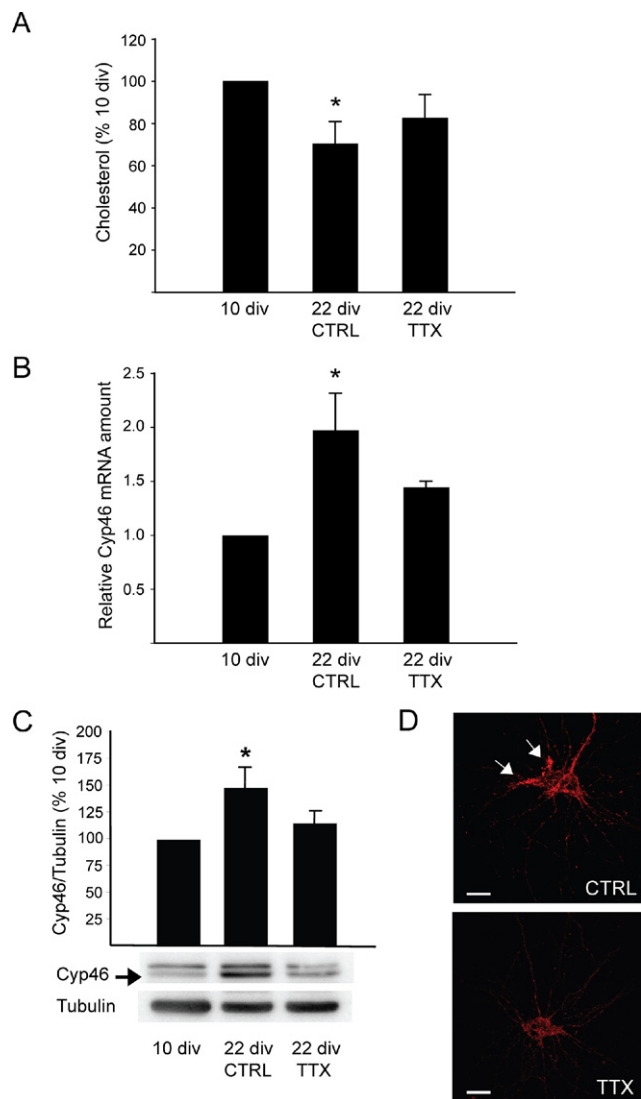
Fig. 6. Inhibition of synaptic activity rescues age-associated cholesterol loss, precludes cholesterol-24-hydroxylase (Cyp46) upregulation and reduces reactive oxygen species (ROS) accumulation in aged neurons. (A) Membrane cholesterol content in 22 days in vitro (DIV) hippocampal neurons, nontreated or chronically treated (14–22 DIV) with tetrodotoxin (TTX), compared with 10 DIV nontreated neurons; *$p < 0.05$. (B) Relative amount of Cyp46 mRNA assessed by quantitative polymerase chain reaction (PCR) in 22 DIV hippocampal neurons, nontreated or chronically treated (14–22 DIV) with TTX, compared with 10 DIV nontreated neurons, whose expression level was considered 1. Cyp46 mRNA levels were normalized to that of β_2-microglobulin; *$p < 0.05$. (C) Expression levels of Cyp46 in membrane extracts of 22 DIV hippocampal neurons, nontreated or chronically treated with TTX, compared with nontreated 10 DIV neurons. Data were normalized to the levels of α-tubulin. A representative western blot is shown below the graph. The arrow indicates the specific band for Cyp46; *$p < 0.05$. (D) Representative confocal images showing the reduction in the intracellular accumulation of ROS measured by dihydrorhodamine staining (red dots indicated by arrows) in 22 DIV hippocampal neurons chronically treated with TTX, compared with nontreated 22 DIV neurons (CTRL). Scale bar: 10 μm. Graphs in (A), (B), and (C) represent mean ± standard error of the mean (SEM) from at least 3 independent experiments.

sion (O'Kane et al., 2003). In fact, western blotting confirmed that the increase in RhoA attached to the plasma membrane that takes place between 10 and 22 DIV was blocked by TTX treatment (Supplementary Fig. 1A). Moreover, we ruled out the toxicity of the treatment by determining apoptosis levels at 22 DIV. The number of apoptotic cells in chronically TTX-treated cultures was not significantly different from controls (20.0 ± 5.0% vs. 15.2 ± 4.4%, respectively; Supplementary Fig. 1B).

3.4. ROS-dependent neurotransmitter mediated cholesterol loss also occurs in synaptic membranes derived from rodent brains

To determine if the mechanism reported above in primary cultured neurons also accounts for a system closer to the in vivo situation, cortex/hippocampal synaptosomes were analyzed for their cholesterol levels in the context of aging and after neurotransmission manipulation. First, we determined the cholesterol content in synaptosomes purified from 4- and 24-month-old mice using Percoll gradients. Fig. 7A shows that the amount of membrane cholesterol in the synaptic membranes of older animals is significantly reduced compared with that of young ones (49.3 ± 6.6%), in agreement with the in vitro data obtained from primary hippocampal cultures. To test if cholesterol loss is also linked to neurotransmission, synaptosomes from young adult rats were depolarized by incubation with 55 mM KCl, which induces massive exocytosis of neurotransmitters (Ghijsen et al., 2003). As expected, this treatment resulted in a significant loss of cholesterol (18.0 ± 6.5%; Fig. 7B). To prove to which extent cholesterol loss could be attributed to the activation of postsynaptic membranes, due to NMDA receptor activation, synaptosomes were incubated with 10 μM NMDA. Although of less magnitude, cholesterol loss was also evident in this case (10.7 ± 2.6%, Fig. 7C). Finally, to determine if synaptic activity produces cholesterol loss via generation of ROS derived from the NADPH oxidase pathway, synaptosomes were pretreated with the ROS inhibitor APC and then incubated with 55 mM KCl. Fig. 7D shows that APC significantly prevented the cholesterol loss induced by depolarization.

4. Discussion

Brain cholesterol levels decrease with age in the human brain (Svennerholm et al., 1991, 1994, 1997) and in mouse hippocampus (Martin et al., 2008). The reduced levels of this sterol are consistent with the age-associated upregulation of the cholesterol hydroxylating enzyme Cyp46 (Lund et al., 1999; Martin et al., 2008). Cholesterol reduction is also evident in embryonic hippocampal neurons undergoing aging in culture (Martin et al., 2008; and present work). The biological consequences of the loss of this sterol, which mainly accounts for the plasma membrane content, are rel-
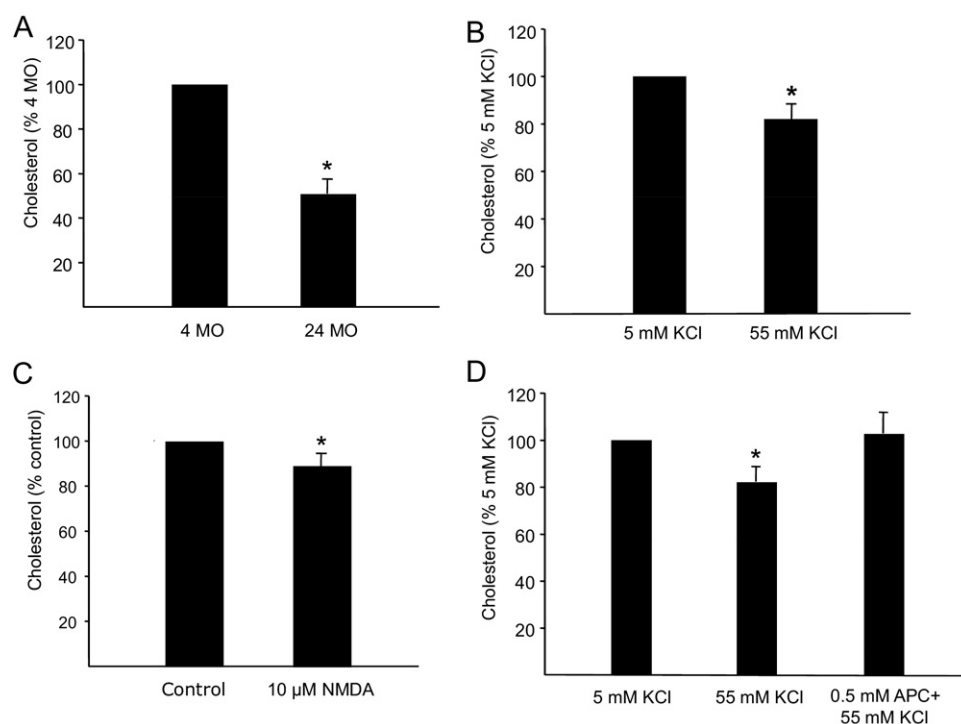
Fig. 7. Synaptic activity induces cholesterol loss through reactive oxygen species (ROS). (A) Membrane cholesterol content in synaptosomes derived from old mice (24 month old [MO]), compared with that of young-adult mice (4 MO). Samples containing equal amount of protein were used for the cholesterol quantification; *$p < 0.05$. (B) Membrane cholesterol content in rat synaptosomes depolarized for 15 minutes with 55 mM KCl, compared with synaptosomes incubated with 5 mM KCl; *$p < 0.05$. (C) Membrane cholesterol content in rat synaptosomes stimulated for 30 minutes with 10 μM N-methyl-D-aspartate (NMDA), compared with nontreated synaptosomes; *$p < 0.05$. (D) Membrane cholesterol content in rat synaptosomes depolarized for 15 minutes with 55 mM KCl, in the absence or presence of 0.5 mM apocynin (APC), compared with synaptosomes incubated with 5 mM KCl; *$p < 0.05$. Graphs in (A), (B), (C), and (D) represent mean $\pm$ standard error of the mean (SEM) from at least 3 independent experiments.

evant. In fact, in addition to its structural importance (membrane rigidity), cholesterol is essential for cell function, through its role in ion permeability and by constituting signaling platforms in the plasma membrane (Tsui-Pierchala et al., 2002). Consistently, we have recently shown that changes like the ones reported here are sufficient to induce a robust activation of a survival response mediated by TrkB, by virtue of the assembly of different lipid-protein rafts (Martin et al., 2008). Naturally, alterations in receptors other than TrkB are expected with membrane cholesterol loss. This awaits future work.

Here, we demonstrate that excitatory synaptic activity is one of the stimuli that induce cholesterol loss in aging neurons in culture. Hence, chronic reduction of electrical activity by TTX prevented cholesterol loss while acute NMDA treatment induced it. The observation that NMDA triggers cholesterol loss, which is precluded by the antagonist AP-5, strongly indicates that chronic TTX treatment prevented cholesterol loss due to reduced glutamatergic neurotransmission. In addition, we confirmed that cholesterol loss produced by acute NMDA treatment is recovered after stimuli (Supplementary Fig. 2). Conversely, if cholesterol loss could not be recovered after stimuli, aged neurons would show a more drastic reduction of this lipid, compro-

mising cell survival. Instead, we propose that a partial recovery after each stimulus would result, in the long term, in the moderate cholesterol loss observed in aged neurons. Although we can confidently say that excitatory neurotransmission is important for cholesterol loss in the "age in the dish" model and synaptosomes, further work is needed to demonstrate if this also occurs in vivo. On the other hand, the observation that TTX treatment only partially prevented age-occurring cholesterol loss indicates that electrical activity is just one of the components involved in the reduction of this sterol. Since we now know that ROS is an important determinant of cholesterol loss, the partial prevention due to TTX should be taken as an indication that other sources of ROS would also affect cholesterol levels during aging. In fact, ROS are unique and therefore their consequences are expected to be the same, irrespective to the generation process involved. Our work also indicates that cholesterol loss during aging due to neurotransmission involves the upregulation of the cholesterol-hydroxylating enzyme Cyp46, in turn due to the production of ROS. Indeed, we provide data showing that synaptic activity increased Cyp46, both at the mRNA and protein levels. Furthermore, this increase can be prevented blocking voltage-gated sodium channels with TTX in cultured hippocampal neurons.

Interestingly, our data reveal not only higher total levels of the enzyme in aged neurons but also a relative increase of its presence at the plasma membrane. The plasma membrane is the cellular site where most of the cell's cholesterol resides (Fisher, 1976; Mondal et al., 2009; Wood et al., 2002) and where Trk receptors are bound by neurotrophins. From now, we would like to propose that the translocation of Cyp46 to the plasma membrane during aging is key for an efficient signaling toward survival and/or plasticity through this receptor, whether directly on the plasma membrane or after internalization into early endosomes.

In a recent work, Nicholson and Ferreira (2009) have reported higher levels of membrane cholesterol in mature cultured hippocampal neurons compared with young ones. A possible explanation for the apparent contradiction with our data are that levels of cholesterol were compared at different days in vitro. While in the mentioned work 7 days was used as reference point for young neurons, in the present work 10 days was the selected reference point. This is an important difference as at 7 days in vitro hippocampal neurons are still in the process of growth, therefore in high demand of new membrane. In agreement with this, we have previously demonstrated that developing neurons have more cholesterol than mature ones (Ledesma et al., 1999). Note-worthy, our results reporting an age-dependent decrease of cholesterol levels find support in vivo, where data obtained from mouse synaptosomes show a clear reduction of this lipid with aging. This would also be consistent with an age-dependent reduction in the fluidity of the neuronal membrane due to, although not exclusively, reduced cholesterol levels (Zs-Nagy, 1994; Yehuda et al., 2002).

The relevance of cholesterol in limiting molecular diffusion has been reported within the synaptic membrane (Renner et al., 2009). Moreover, mice lacking Cyp46 show impaired learning and hippocampal long term potentiation because of deficits in cholesterol turnover (Kotti et al., 2006). Although we have recently showed that TrkB activation during aging is critical for neuronal survival under stress (Martin et al., 2009), it is quite reasonable that cholesterol loss induced by synaptic activity would greatly affect synapse stability and therefore synaptic performance. Research on this matter will contribute to understand the role, until now neglected, of lipids in neuronal functionality.

Disclosure statement

There are no actual or potential conflicts of interest. The appropriate institutional approval for all animal experiments was obtained.

Acknowledgements

Appendix. Supplementary data

Supplementary data associated with this article can be found, in the online version, at doi:10.1016/j.neurobiolaging. 2010.06.001.

References

Aksenova, M.V., Aksenov, M.Y., Markesbery, W.R., Butterfield, D.A., 1999. Aging in a dish: age-dependent changes of neuronal survival, protein oxidation, and creatine kinase BB expression in long-term hippocampal cell culture. J. Neurosci. Res. 58, 308–317.

An, W.L., Cowburn, R.F., Li, L., Braak, H., Alafuzoff, I., Iqbal, K., Iqbal, I.G., Winblad, B., Pei, J.J., 2003. Up-regulation of phosphorylated/ activated p70 S6 kinase and its relationship to neurofibrillary pathology in Alzheimer's disease. Am. J. Pathol. 163, 591–607.

Attwell, D., Iadecola, C., 2002. The neural basis of functional brain imaging signals. Trends Neurosci. 25, 621–625.

Bacci, A., Verderio, C., Pravettoni, E., Matteoli, M., 1999. Synaptic and intrinsic mechanisms shape synchronous oscillations in hippocampal neurons in culture. Eur. J. Neurosci. 11, 389–397.

Behrens, M.M., Ali, S.S., Dao, D.N., Lucero, J., Shekhtman, G., Quick, K.L., Dugan, L.L., 2007. Ketamine-induced loss of phenotype of fast-spiking interneurons is mediated by NADPH-oxidase. Science 318, 1645–1647.

Björkhem, I., Lütjohann, D., Diczfalusy, U., Ståhle, L., Ahlborg, G., Wahren, J., 1998. Cholesterol homeostasis in human brain: turnover of 24S-hydroxycholesterol and evidence for a cerebral origin of most of this oxysterol in the circulation. J. Lipid Res. 39, 1594–1600.

Brennan, A.M., Suh, S.W., Won, S.J., Narasimhan, P., Kauppinen, T.M., Lee, H., Edling, Y., Chan, P.H., Swanson, R.A., 2009. NADPH oxidase is the primary source of superoxide induced by NMDA receptor activation. Nat. Neurosci. 12, 857–863.

Chen, Q.M., Bartholomew, J.C., Campisi, J., Acosta, M., Reagan, J.D., Ames, B.N., 1998. Molecular analysis of H2O2-induced senescent-like growth arrest in normal human fibroblasts: p53 and Rb control G1 arrest but not cell replication. Biochem. J. 332, 43–50.

Dröge, W., Schipper, H.M., 2007. Oxidative stress and aberrant signaling in aging and cognitive decline. Aging Cell 6, 361–370.

Dunkley, P.R., Heath, J.W., Harrison, S.M., Jarvie, P.E., Glenfield, P.J., Rostas, J.A., 1988. A rapid Percoll gradient procedure for isolation of synaptosomes directly from an S1 fraction: homogeneity and morphology of subcellular fractions. Brain Res. 441, 59–71.

Fifkova, E., Morales, M., 1992. Aging and the neurocytoskeleton. Exp. Gerontol. 27, 125–136.

Fisher, K.A., 1976. Analysis of membrane halves: cholesterol. Proc. Natl. Acad. Sci. U. S. A. 73, 173–177.

Ghijsen, W.E.J.M., Leenders, A.G.M., Lopes da Silva, F.H., 2003. Regulation of vesicle traffic and neurotransmitter release in isolated nerve terminals. Neurochem. Res. 28, 1443–1452.

Gooney, M., Messaoudi, E., Maher, F.O., Bramham, C.R., Lynch, M.A., 2004. BDNF-induced LTP in dentate gyrus is impaired with age: analysis of changes in cell signaling events. Neurobiol. Aging 25, 1323–1331.

Gray, D.A., Woulfe, J., 2005. Lipofuscin and aging: a matter of toxic waste. Sci. Aging Knowledge Environ. 2005(5), re1.

Hattiangady, B., Rao, M.S., Shetty, G.A., Shetty, A.K., 2005. Brain-derived neurotrophic factor, phosphorylated cyclic AMP response element binding protein and neuropeptide Y decline as early as middle age in the dentate gyrus and CA1 and CA3 subfields of the hippocampus. Exp. Neurol. 195, 353–371.

Kaech, S., Banker, G., 2006. Culturing hippocampal neurons. Nat. Protoc. 1, 2406–2415.

Kamsler, A., Segal, M., 2004. Hydrogen peroxide as a diffusible signal molecule in synaptic plasticity. Mol. Neurobiol. 29, 167–178.

Köller, H., Siebler, M., Müller, H.W., 1993. Paroxysmal long-lasting depolarizations in cultured hippocampal neurons are generated by activation of NMDA and non-NMDA receptors. Synapse 14, 214–220.

Kotti, T.J., Ramirez, D.M.O., Pfeiffer, B.E., Huber, K.M., Russel, D.W., 2006. Brain cholesterol turnover required for geranylgeraniol production and learning in mice. Proc. Natl. Acad. Sci. U. S. A. 103, 3869–3874.

Kuroda, Y., Kobayashi, K., Ichikawa, M., Kawahara, M., Muramoto, K., 1995. Application of long-term cultured neurons in aging and neurological research: aluminum neurotoxicity, synaptic degeneration and Alzheimer's disease. Gerontology 41, 2–6.

Ledesma, M.D., Brügger, B., Bünning, C., Wieland, F.T., Dotti, C.G., 1999. Maturation of the axonal plasma membrane requires upregulation of sphingomyelin synthesis and formation of protein-lipid complexes. EMBO J. 18, 1761–1771.

Lund, E.G., Guileyardo, J.M., Russell, D.W., 1999. cDNA cloning of cholesterol 24-hydroxylase, a mediator of cholesterol homeostasis in the brain. Proc. Natl. Acad. Sci. U. S. A. 96, 7238–7243.

Lütjohann, D., Breuer, O., Ahlborg, G., Nennesmo, I., Siden, A., Diczfalusy, U., Björkhem, I., 1996. Cholesterol homeostasis in human brain: evidence for an age-dependent flux of 24S-hydroxycholesterol from the brain into the circulation. Proc. Natl. Acad. Sci. U. S. A. 93, 9799–9804.

Martin, M.G., Perga, S., Trovò, L., Rasola, A., Holm, P., Rantamäki, T., Harkany, T., Castrén, E., Chiara, F., Dotti, C.G., 2008. Cholesterol loss enhances TrkB signaling in hippocampal neurons aging in vitro. Mol. Biol. Cell 19, 2101–2112.

Martin, M.G., Trovò, L., Perga, S., Sadowska, A., Rasola, A., Chiara, F., Dotti, C.G., 2009. Cyp46-mediated cholesterol loss promotes survival in stressed hippocampal neurons. Neurobiol. Aging, Epub ahead of print. doi:10.1016/j.neurobiolaging.2009.04.022.

Mondal, M., Mesmin, B., Mukherjee, S., Maxfield, F.R., 2009. Sterols are mainly in the cytoplasmic leaflet of the plasma membrane and the endocytic recycling compartment in CHO cells. Mol. Biol. Cell 20, 581–588.

Nicholson, A.M., Ferreira, A., 2009. Increased membrane cholesterol might render mature hippocampal neurons more susceptible to beta-amyloid-induced calpain activation and tau toxicity. J. Neurosci. 29, 4640–4651.

O'Kane, E.M., Stone, T.W., Morris, B.J., 2003. Activation of Rho GTPases by synaptic transmission in the hippocampus. J. Neurochem. 87, 1309–1312.

Ohyama, Y., Meaney, S., Heverin, M., Ekström, L., Brafman, A., Shafir, M., Andersson, U., Olin, M., Eggertsen, G., Diczfalusy, U., Feinstein, E., Björkhem, I., 2006. Studies on the transcriptional regulation of cholesterol 24-hydroxylase (CYP46A1): marked insensitivity toward different regulatory axes. J. Biol. Chem. 281, 3810–3820.

Perez, M., Santa-Maria, I., Gomez de Barreda, E., Zhu, X., Cuadros, R., Cabrero, J.R., Sanchez-Madrid, F., Dawson, H.N., Vitek, M.P., Perry, G., Smith, M.A., Avila, J., 2009. Tau an inhibitor of deacetylase HDAC6 function. J. Neurochem. 109, 1756–1766.

Pham, C.G., Papa, S., Bubici, C., Zazzeroni, F., Franzoso, G., 2005. Oxygen JNKies: phosphatases overdose on ROS. Dev. Cell 8, 452–454.

Pikkarainen, M., Kauppinen, T., Alafuzoff, I., 2009. Hyperphosphorylated tau in the occipital cortex in aged nondemented subjects. J. Neuropathol. Exp. Neurol. 68, 653–660.

Porter, N.M., Thibault, O., Thibault, V., Chen, K.-C., Landfield, P.W., 1997. Calcium channel density and hippocampal cell death with age in long-term culture. J. Neurosci. 17, 5629–5639.

Renner, M., Choquet, D., Triller, A., 2009. Control of the postsynaptic membrane viscosity. J. Neurosci. 29, 2926–2937.

Schubert, V., Da Silva, J.S., Dotti, C.G., 2006. Localized recruitment and activation of RhoA underlies dendritic spine morphology in a glutamate receptor-dependent manner. J. Biol. Chem. 172, 453–467.

Serrano, F., Klann, E., 2004. Reactive oxygen species and synaptic plasticity in the aging hippocampus. Ageing Res. Rev. 3, 431–443.

Shetty, A.K., Rao, M.S., Hattiangady, B., Zaman, V., Shetty, G.A., 2004. Hippocampal neurotrophin levels after injury: Relationship to the age of the hippocampus at the time of injury. J. Neurosci. Res. 78, 520–532.

Small, S.A., Duff, K., 2008. Linking Abeta and tau in late-onset Alzheimer's disease: a dual pathway hypothesis. Neuron 60, 534–542.

Svennerholm, L., Boström, K., Helander, C.G., Jungbjer, B., 1991. Membrane lipids in the aging human brain. J. Neurochem. 56, 2051–2059.

Svennerholm, L., Boström, K., Jungbjer, B., Olsson, L., 1994. Membrane lipids of adult human brain: lipid composition of frontal and temporal lobe in subjects of age 20 to 100 years. J. Neurochem. 63, 1802–1811.

Svennerholm, L., Boström, K., Jungbjer, B., 1997. Changes in weight and compositions of major membrane components of human brain during the span of adult human life of Swedes. Acta Neuropathol. 94, 345–352.

Szweda, P.A., Camouse, M., Lundberg, K.C., Oberley, T.D., Szweda, L.I., 2003. Aging, lipofuscin formation, and free radical-mediated inhibition of cellular proteolytic systems. Ageing Res. Rev. 2, 383–405.

Tomobe, K., Nomura, Y., 2009. Neurochemistry, neuropathology, and heredity in SAMP8: a mouse model of senescence. Neurochem. Res. 34, 660–669.

Tsui-Pierchala, B.A., Encinas, M., Milbrandt, J., Johnson, E.M., Jr, 2002. Lipid rafts in neuronal signaling and function. Trends Neurosci. 25, 412–417.

Uboga, N.V., Price, J.L., 2000. Formation of diffuse and fibrillar tangles in aging and early Alzheimer's disease. Neurobiol. Aging 21, 1–10.

Urenjak, J., Obrenovitch, T.P., 1996. Pharmacological modulation of voltage-gated Na$^+$ channels: a rational and effective strategy against ischemic brain damage. Pharmacol. Rev. 48, 21–67.

Wood, W.G., Schroeder, F., Igbavboa, U., Avdulov, N.A., Chochina, S.V., 2002. Brain membrane cholesterol domains, aging and amyloid beta-peptides. Nerobiol. Aging 23, 685–694.

Wu, C., Miloslavskaya, I., Demontis, S., Maestro, R., Galaktionov, K., 2004. Regulation of cellular response to oncogenic and oxidative stress by Seladin-1. Nature 432, 640–645.

Yehuda, S., Rabinovitz, S., Carasso, R.L., Mostofsky, D.I., 2002. The role of polyunsaturated fatty acids in restoring the aging neuronal membrane. Neurobiol. Aging 23, 843–853.

Zs-Nagy. I, 1994. The Membrane Hypothesis of Aging. CRC Press, Boca Raton, FL.

Zucker, R.S., 1999. Calcium-and activity-dependent synaptic plasticity. Curr. Opin. Neurobiol. 9, 305–313.